

Diagnosis of Acute Cerebral Infarction: Comparison of CT and MR Imaging

R. Nick Bryan¹
 Lucien M. Levy¹
 Warren D. Whitlow¹
 James M. Killian²
 Thomas J. Preziosi³
 Joana A. Rosario¹

The appearance of acute cerebral infarction was evaluated on MR images and CT scans obtained in 31 patients within 24 hr of the ictus; follow-up examinations were performed 7–10 days later in 20 of these patients and were correlated with the initial studies. Acute infarcts were visible more frequently on MR images than on CT scans (82% vs 58%). Proton density- and T2-weighted scans usually demonstrated regions of hyperintensity corresponding to acute infarcts, but proton density-weighted scans often showed better definition of the lesion in terms of regional anatomy. Follow-up MR images and CT scans identified approximately 88% of subacute strokes, 54% of which were better defined and/or larger than on the initial examination. In 20% of lesions, “hemorrhagic” characteristics were seen on at least one examination. CT and MR imaging were comparable in delineating acute hemorrhage, but MR detected more cases with evidence of hemorrhage on follow-up examinations.

MR appears to be more sensitive than CT in the imaging of acute stroke.

AJNR 12:611–620, July/August 1991; *AJR* 157: September 1991

Although the pathophysiology and diagnosis of stroke have been studied by numerous imaging techniques [1–3], none currently enable precise diagnosis and delineation of acute cerebral infarction. The diagnosis of acute stroke is based primarily on the clinical observation of an acute neurologic deficit and the exclusion of other diagnostic possibilities by CT scanning and metabolic tests [4]. CT often appears normal in the first 24–48 hr [5–8], and may not establish a definitive diagnosis. Physiologic imaging tests such as xenon CT or single-photon emission CT may detect early cerebral perfusion abnormalities that are related to, but not the same as, infarction [9]. Furthermore, these studies have low spatial resolution compared with CT and MR imaging and may be logistically complicated. More sophisticated physiologic imaging examinations such as positron-emission tomography often are not available or practical [10]. MR has been used to evaluate stroke in animal models [11–15], and some studies have reported on MR of stroke in humans [16–22]. Our investigation evaluates the appearance of early stroke on MR, and compares the sensitivities of MR and CT in the detection of this disease.

Subjects and Methods

This prospective study consisted of two parts. First, MR and CT scans were obtained within 24 hr of ictus in patients with a clinical diagnosis of acute stroke. We used the standard clinical criteria for acute stroke, the basis of which is the presentation of a new, measurable neurologic deficit within the previous 24 hr that persists at least 24 hr [4]. Such clinical criteria are estimated to be 90% sensitive. While not definitive, these criteria are often used as a clinical gold standard. Included in this diagnosis would be thrombotic and/or embolic and hemorrhagic or nonhemorrhagic stroke. Subarachnoid hemorrhage usually would not be included. Other selection criteria included willingness of the patients to undergo initial and follow-up CT and MR, their ability to give informed consent, and instrument availability. No

Received July 23, 1990; returned for revision October 1, 1990; revision received January 10, 1991; accepted January 21, 1991.

This work was supported in part by National Institutes of Health grant NS 19056-06.

¹Neuroradiology Division, Meyer 8-140, The Russell H. Morgan Department of Radiology and Radiological Science, The Johns Hopkins Hospital, 600 N. Wolfe St., Baltimore, MD 21205. Address reprint requests to R. N. Bryan.

²Department of Neurology, Baylor College of Medicine, Houston, TX 77030.

³Department of Neurology, The Johns Hopkins Hospital, Baltimore, MD 21205.

0195-6108/91/1204-0611

© American Society of Neuroradiology

more than one patient could be in the protocol at any time. Therefore, patients were entered approximately every 2 weeks on a "first-to-fill" basis. Between 1987 and 1989, 44 patients were entered into the protocol. Nine did not complete one or more imaging studies within 24 hr of ictus and were excluded from further analysis. In four others, a final clinical diagnosis of stroke was not made. Fifteen women and 16 men 15–94 years old (median age, 63) with a final diagnosis of stroke completed the first part of the protocol. Twenty of these patients participated in the second part of the study, which consisted of follow-up CT (19 patients) and MR (20 patients) examinations performed 7–10 days following the acute episode. Eleven patients were unable or refused to undergo the second set of examinations despite initial agreement to do so.

Although entry into the study was determined by the initial clinical diagnosis, inclusion in the Results portion of this report was determined by the neurologic discharge diagnosis, which was confirmed by either of the neurologists participating in this study. These neurologists were not the primary attending physicians and did not know the results of the imaging studies.

The CT scans on admission were unenhanced, whereas the follow-up scans were obtained with and without enhancement. CT scans were obtained on either a GE 9800 (General Electric Medical Systems, Milwaukee, WI) or a Siemens DR3 (Siemens Medical Systems Group, Iselin, NJ) scanner with a slice thickness 4–5 mm through the posterior fossa and 8–10 mm supratentorially. MR studies followed the CT examinations as required by the Institutional Review Board. MR examinations included proton density-weighted, 3000–3500/22–35 (TR/TE); T2-weighted, 3000–3500/80–120; and T1-weighted, 500–600/20–35, spin-echo sequences. MR scans were obtained on Siemens 0.5- and 1.0-T and General Electric 1.5-T instruments. All scans were in the axial projection and consisted of 5-mm-thick slices with a 2.0- or 2.5-mm gap, 256 × 256 matrix, and one acquisition for 1.0- and 1.5-T double-echo sequences and two acquisitions for the 0.5-T system. For T1-weighted sequences, four acquisitions were used at 0.5 T and two at 1.0 and 1.5 T. In 16 cases, gradient-echo (GRE) scans, 500/30/90° (TR/TE/flip angle) and 30/15/10°, also were obtained to evaluate T2* effects.

The imaging studies were separated into two sets, initial and follow-up examinations. Film identification was blinded, and the pseudo-randomized (as to patient, type of examination, and date) examinations were presented independently to two observers (both neuroradiologists) for interpretation. The interpreters determined the presence or absence of an acute stroke on the usual clinical basis of a focal region of radiolucency (or increased radiodensity if hemorrhagic) in a vascular pattern on CT with "appropriate" (usually mild) mass effect. On MR studies, the criteria were similar except for the substitution of increased signal intensity on proton density- and T2-weighted images for the radiolucency seen on CT. Lesions were recorded as to location (cortical, subcortical, and posterior fossa, as well as specific regions), size (0–2, 2–5, and >5 cm), and radiodensity and signal intensity (increased, normal, decreased) on CT and MR images, respectively. Clinical information was not initially available for review. For statistical purposes, the locations of the lesions (right vs left hemisphere) seen on MR and CT follow-up studies were used as the gold standard for determining the sensitivity and specificity of both techniques in the initial examination. Each of the 40 hemispheres in the 20 patients who underwent follow-up examinations was treated as a separate entity.

A second interpretation was conducted that compared the initial and follow-up images of each patient as to the location, size, and signal intensity of the lesion. The examinations were interpreted jointly on a third occasion with the addition of clinical information. This resulted in a consensus opinion, which was used for descriptive findings.

Results

Of the 31 patients with acute stroke who underwent initial CT and MR scans, 13 had cerebral cortical strokes, eight had subcortical lesions, seven had combined cortical and subcortical lesions, and three had posterior fossa strokes. The mean time between ictus and CT was 8 hr; between ictus and MR, 12 hr. The numbers and percentages of strokes diagnosed by each of the observers on initial and follow-up CT and MR scans are shown in Table 1. Table 2 shows the percent agreement between the observers. On the basis of the mean of the multiobserver observations of the 31 initial studies, 58% of the initial CT examinations were thought to show an acute stroke as compared with 82% on MR. For the statistical computation of the sensitivity (CT = 59.1%, MR = 88.7%) and specificity for diagnosis of acute stroke (CT = 100%, MR = 91.7%), the combined results of the two interpreters were used only when both initial and follow-up studies had been performed. To determine whether the differences in those values were statistically significant, a chi-square test was applied for both sensitivity (χ^2 , 1 df = 7.06) and specificity (χ^2 , 1 df = 1.56). At a confidence level of 95% ($\chi^2 = .95$, 1 df = 3.84), there was a statistically significant difference in the sensitivities of CT scanning as compared with MR for the detection of acute stroke. That difference did not hold for specificity.

On the initial MR scans, proton density- or T2-weighted images showed the lesions as areas of increased signal intensity in 25 cases (Table 3, Fig. 1). Signal intensities were increased on both proton density- and T2-weighted images in 22 cases. In two cases in which the proton-density signal intensity was increased and the T2 signal intensity was thought to be normal, both lesions were cortical. In one case (a pontine lesion), the proton-density signal intensity was normal and the T2 signal intensity was increased. Proton

TABLE 1: CT and MR Studies Diagnosed as Showing Acute Stroke

Observer No./Study	No. Diagnosed/Total No. (%)	
	Initial Studies	Follow-up Studies
1		
CT	21/31 (68)	16/19 (84)
MR	27/31 (87)	19/20 (95)
2		
CT	15/31 (48)	15/19 (79)
MR	24/31 (77)	19/20 (95)
Mean value		
CT	(58)	(82)
MR	(82)	(95)

TABLE 2: Percentage Agreement Between the Two Observers in Interpreting Initial and Follow-up CT and MR Studies in Acute Stroke

Imaging Method	Study Interval	
	Initial	Follow-up
CT	81%	95%
MR	94%	100%

density-weighted images appeared to show slightly better contrast between the lesion and its surroundings than T2-weighted images did. In six cases, neither the proton-density nor the T2 signal intensity was increased. In two of these cases, T2-weighted images showed decreased signal inten-

TABLE 3: Signal Intensity of Stroke Lesions (Compared with Normal Hemisphere) on MR Sequences

Examination/ Signal Intensity	PDW	T2W	T1W	GRE
Initial (<i>n</i> = 31)				
Increased	24	22	2	0
Isointense	7	7	25	14
Decreased	0	2	4	2
Follow-up (<i>n</i> = 20)				
Increased	17	17	6	2
Isointense	2	2	9	11
Decreased	1	1	5	1

Note.—PDW = proton-density weighted; T2W = T2 weighted; T1W = T1 weighted; GRE = gradient echo.

sity indicative of acute hemorrhage. In both cases there was a corresponding decrease in signal intensity on GRE scans plus an increased radiodensity on CT scans. Both these lesions were typical basal ganglia hematomas approximately 2–3 cm in diameter (Fig. 2). T1-weighted images were the least sensitive in the detection of stroke. On initial examination, only six cases were abnormal, four showing decreased signal intensity and two showing increased signal intensity.

On follow-up CT, a mean of 82% of the examinations were thought to show the stroke regions; interobserver variability was minimal. On follow-up MR scans, 95% (19/20) of the lesions were seen and there was no interobserver variability. Of the 20 lesions seen on follow-up MR, 17 were reflected by increased signal intensity on proton density- and T2-weighted images, while decreased signal intensity was seen on proton density- and T2-weighted images in one case. In the latter case, decreased signal intensity was seen on GRE scans also. Two lesions were isointense on proton density- and T2-weighted images. On T1-weighted images, increased signal

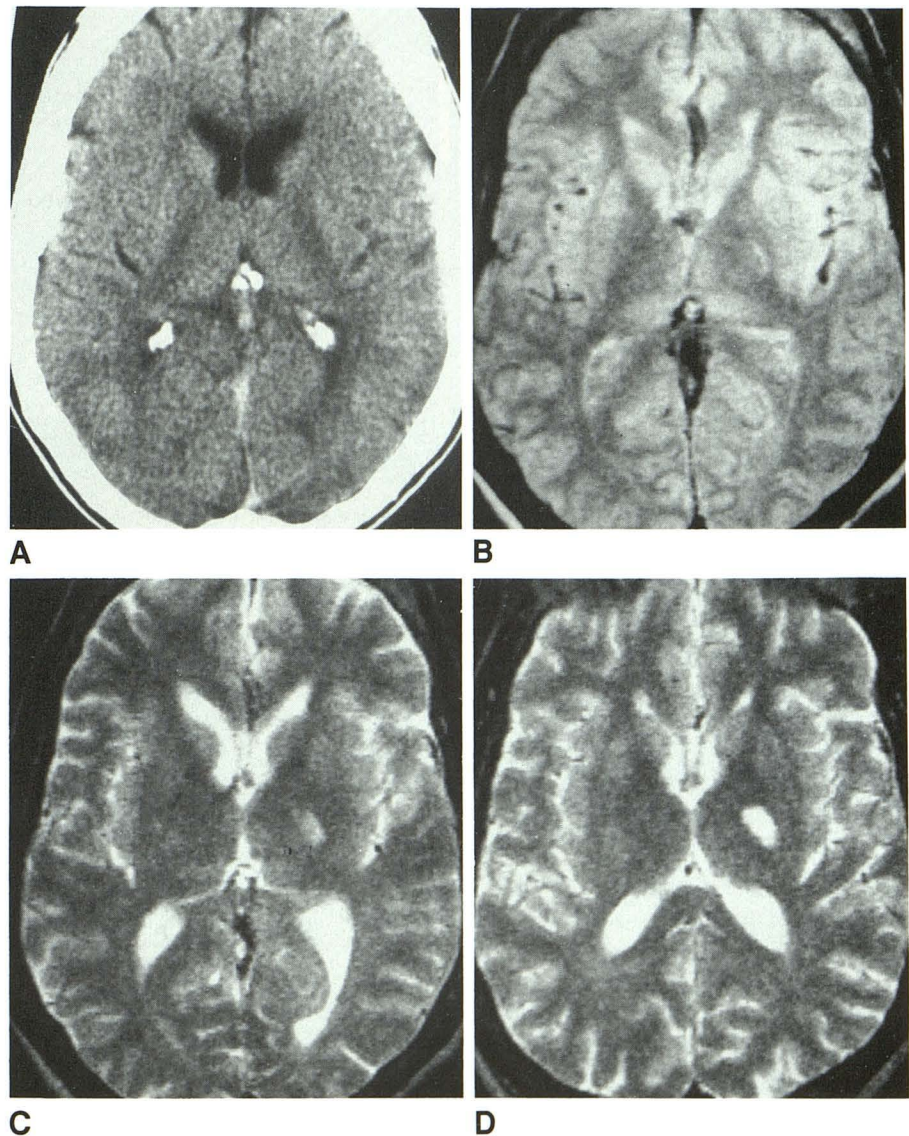


Fig. 1.—Infarct in left posterior limb of internal capsule.

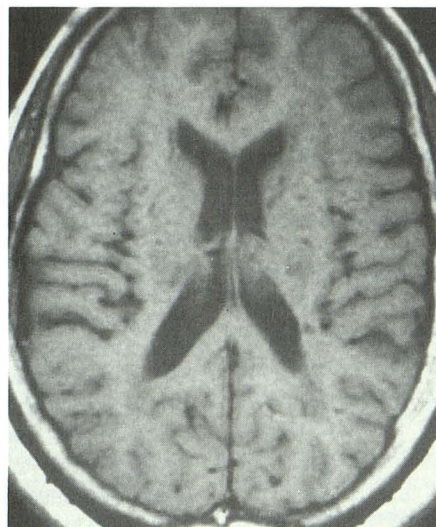
A, CT scan 6 hr after ictus is normal.

B and C, Proton density-(3000/35) and T2-(3000/105) weighted MR images show infarct as area of increased signal intensity.

D, T2-weighted MR image (3000/105) obtained 7 days after ictus shows better definition of lesion, which is slightly enlarged.



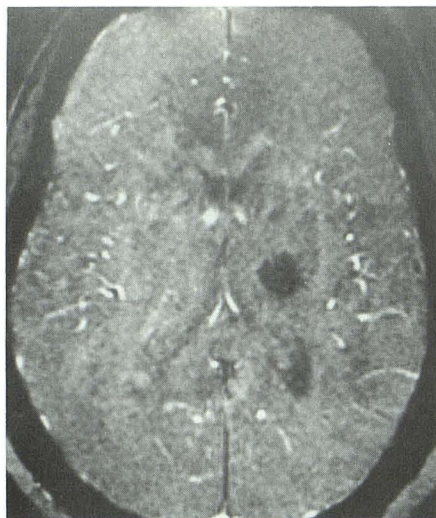
A



B



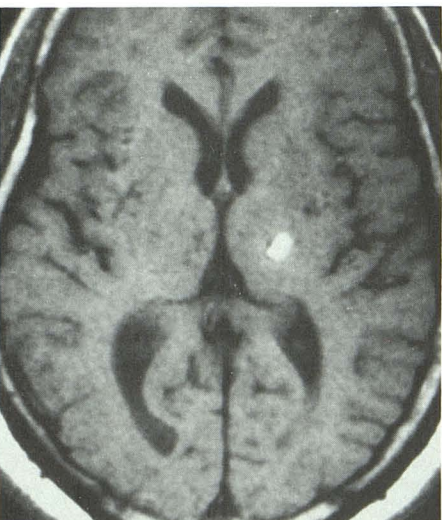
C



D



E



F



G

Fig. 2.—Hematoma in left basal ganglia at 1 (A–D) and 12 (E–G) days.

A, CT scan shows left basal ganglia hematoma.

B, T1-weighted MR image (500/20). Hematoma is isointense.

C, T2-weighted MR image (3000/100) shows decreased signal intensity in center of hematoma and increased signal in periphery.

D, GRE image (33/17/30°) shows hematoma has markedly decreased signal intensity.

E, Follow-up CT scan shows hematoma to be hypointense.

F, T1-weighted MR image (500/20) shows increased signal intensity.

G, GRE image (33/17/30°) shows increased signal intensity in hematoma. (Additional lesions in right thalamus and basal ganglia presumably are previous vascular insults.)

intensity was seen in six lesions while decreased signal intensity was seen in five.

Owing to the nonquantitative evaluation of lesion size, only relative estimates of size and progression could be made (Table 4). On the basis of consensus MR interpretations, 10

lesions initially were 0–2 cm in maximum diameter, nine were 2–5 cm, and seven were larger than 5 cm. In 21 cases in which the same lesions were visible on initial CT and MR studies, the lesions subjectively appeared to be larger on MR in six cases (Fig. 3). Progression in lesion size is probably best assessed by comparing only those lesions in which both initial and follow-up MR studies were performed. Of these 16 cases, four lesions appeared to enlarge, three diminished, and nine showed no change in size.

The CT criterion for the presence of "hemorrhage" was increased radiodensity relative to gray matter. On MR, the criteria for hemorrhage were decreased signal intensity on T2-weighted images, increased signal intensity on T1-weighted images, and/or decreased signal intensity on GRE images, all relative to normal white matter.

There was good agreement among observers as to the presence or absence of hemorrhage (Table 5). On initial studies, both interpreters agreed on the presence of two basal ganglia hematomas that were reflected by increased density on CT and decreased signal intensity on T2-weighted and GRE images. There was also agreement about an acute hemorrhagic infarct in the basal ganglia, reflected by increased signal intensity on T1-weighted images (Fig. 4). However, on one CT and one MR examination there was disagreement as

TABLE 4: Size of Stroke Lesions and Apparent Change in Size on Follow-up Scans

Study/Lesion Size (cm)	Initial Study (No.)	Follow-up Study (No.)			
		Larger	Smaller	No Change	No Follow-up
CT					
0–2	9	5	1	2	1
2–5	8	2	2	0	4
>5	4	0	0	1	3
Not seen	10	3	0	3	4
Total	31	10	3	6	12
MR					
0–2	10	2	0	3	5
2–5	9	2	2	1	4
>5	7	0	1	5	1
Not seen	5	3	0	1	1
Total	31	7	3	10	11

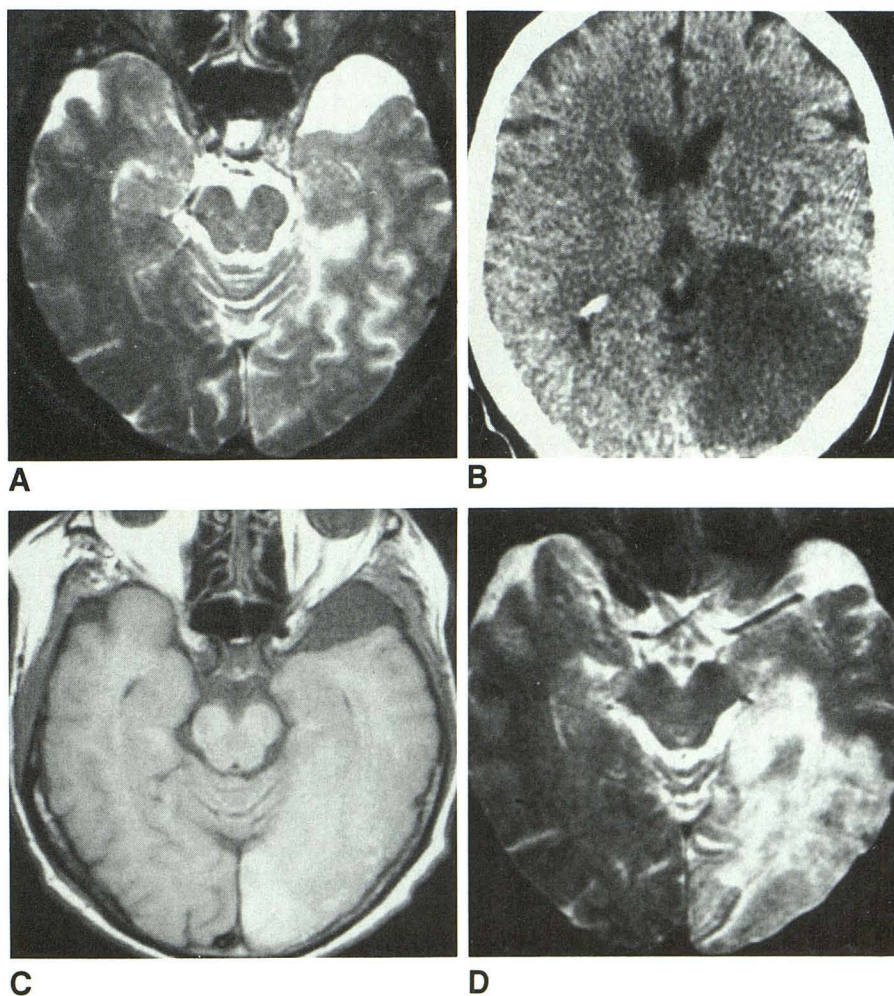


Fig. 3.—Infarct in left occipital lobe at 1 (A) and 7 (B–D) days appears hemorrhagic and larger on follow-up examinations.

A, T2-weighted MR image (3000/100) shows left occipital lobe infarct with increased signal intensity.

B, Follow-up CT scan shows large infarct.

C, T1-weighted MR image (500/20) shows evidence of hemorrhage with increased signal intensity.

D, T2-weighted MR image (3000/100) shows apparent growth of infarct since initial examination. (Incidental arachnoid cyst in left middle fossa.)

to the presence of hemorrhage. In these cases, the infarcts were radiolucent on CT and showed increased signal intensity on T2-weighted images; however, questionable intermixed regions of increased radiodensity on CT and/or decreased signal intensity on T1-weighted images were seen also. On follow-up examinations, there was disagreement concerning hemorrhage on one CT scan and no disagreement on MR scans.

TABLE 5: Findings of the Observers Concerning the Presence or Absence of Hemorrhagic Infarct on CT and MR

Study/Finding	CT	MR
Initial		
Present	2	3
Absent	28	27
Indeterminate	1	1
Total	31	31
Follow-up		
Present	2	6
Absent	16	14
Indeterminate	1	0
Total	19	20

Note.—Findings are listed as present or absent if the observers agreed on the finding. If the observers disagreed, the finding is listed as indeterminate.

The main discord between CT and MR evidence of hemorrhage was seen in follow-up studies, in which four cases of hemorrhagic signal on MR were reflected by increased signal intensity on T1-weighted images without evidence of increased radiodensity on either the initial or follow-up CT study (Figs. 3 and 4). In none of these four cases was there decreased signal intensity on initial or follow-up T2-weighted or GRE scans. The percentage agreement between the two observers for the detection of hemorrhage varied little between the initial (CT, 97%; MR, 97%) and follow-up (CT, 95%; MR, 100%) studies.

Discussion

Acute infarcts are visible more often on MR than on CT scans. On admission, 82% of MR scans showed abnormality as compared with 58% of CT scans. On follow-up scans, approximately 90% of both CT and MR scans were abnormal. In the one instance in which a "stroke" was detected by CT and not seen on MR, the lesion was a small cortical subarachnoid hemorrhage (Fig. 5). This case illustrates the known limitations of MR in detecting subarachnoid hemorrhage.

This report raises the question of diagnostic criteria. Two were used in the present case. First, for protocol entry and

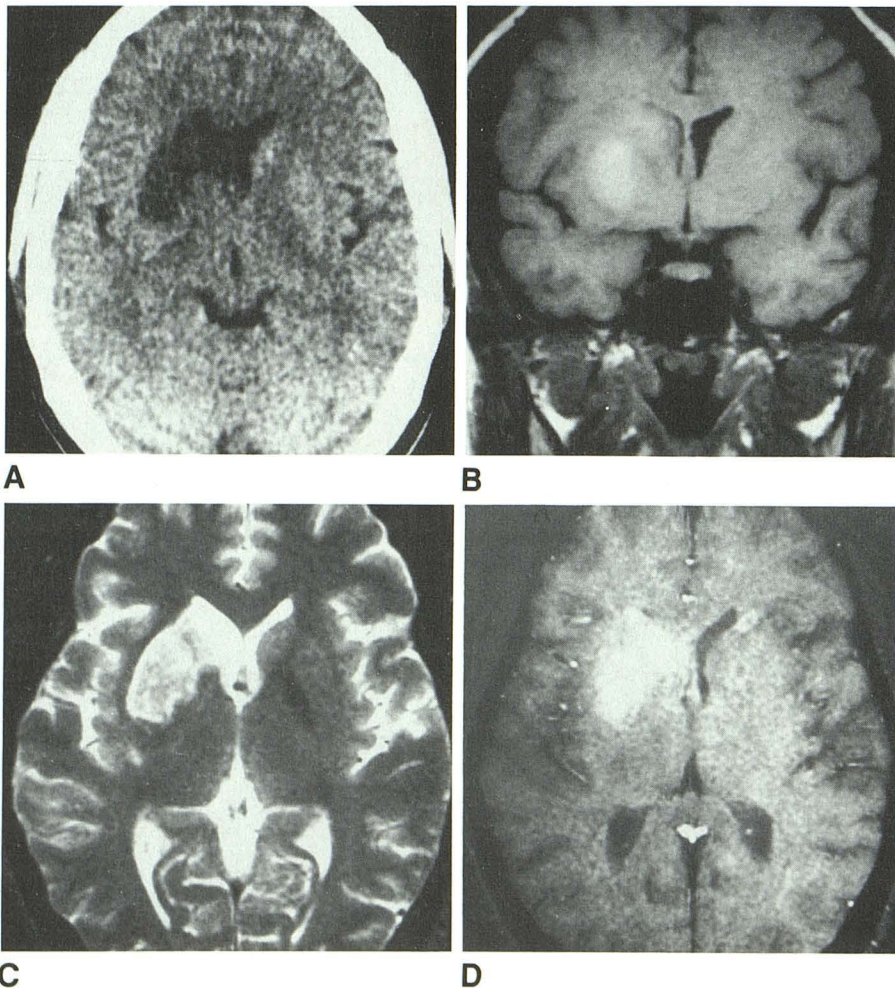


Fig. 4.—Infarct in right basal ganglia shows hemorrhage on MR but not on CT on day 1.

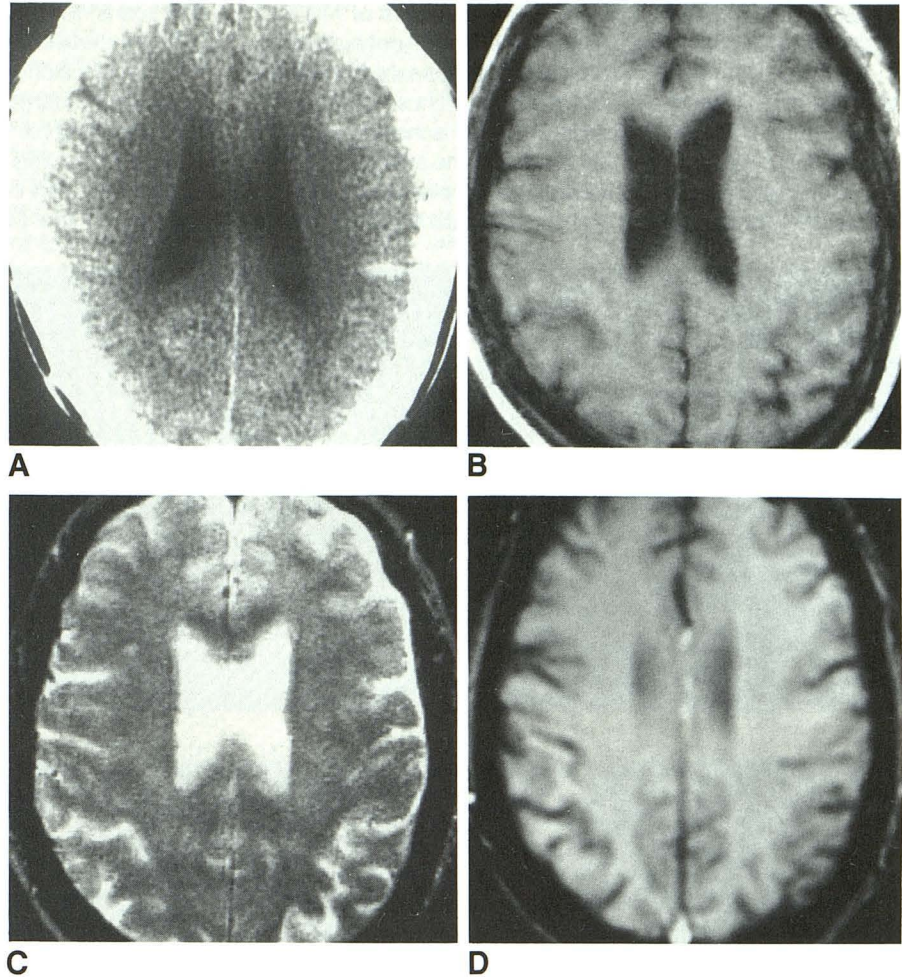
A, CT shows right basal ganglia infarct.
B, T1-weighted coronal MR image (500/20) shows increased signal intensity suggesting hemorrhage.

C and **D**, T2-weighted, 3000/100 (**C**), and GRE, 33/17/30° (**D**), images show infarct but no signal changes definitive of acute hematoma, although heterogeneous signal intensity in lesion on T2-weighted image might raise such a possibility.

Fig. 5.—Small left cortical subarachnoid hemorrhage was seen on initial CT but not on MR.

A, CT scan shows small left cortical subarachnoid hemorrhage.

B–D, T1-weighted, 500/20 (B); T2-weighted, 3000/100 (C); and GRE, 33/17/30° (D), images are all normal.



descriptive results, we used clinical criteria for stroke diagnosis. This approach is imprecise, but is required for a prospective study since there is no accepted, definitive test for stroke prior to imaging studies. For statistical analysis of sensitivity and specificity, we have restricted our analysis to those cases with a clinical diagnosis of stroke and an abnormal follow-up imaging study. This possibly increases the sensitivity and specificity of CT and MR, since patients with stroke that was not seen on imaging studies (false negative) would be excluded from analysis. Our results and previous reports would suggest that less than 5% of stroke patients fall into this category [5, 6, 8].

Even when possible, the diagnosis of early stroke on CT is often relatively difficult, as the radiographic findings—radiolucency and mass—may be quite subtle, making the diagnosis tentative [8]. This difficulty in diagnosis is reflected in the significant interobserver variability in interpretation of the initial CT scans. This variability nearly disappeared on follow-up scans, by which time the lesions had become obvious.

The CT scans that were abnormal on the first examination appeared to underestimate the size of the lesion as compared with MR, but we have not quantified this discrepancy. The general sensitivity of CT may be higher than observed in this study, since severely ill and uncooperative patients were negatively biased for selection. A high rate of abnormal CT

(and MR) findings probably would have been found in such patients. The 58% mean rate for CT in the early detection of stroke is less than that in some other reports [7, 8]. However, no previous reports were prospective studies with blinded interpretations.

On MR imaging, regions of increased signal intensity due to acute infarcts were usually observed on both proton density- and T2-weighted images. The changes on proton density-weighted images were subjectively more conspicuous in three cases. This finding was particularly evident for portions of strokes involving peripheral gray matter. In addition, when structures such as the internal and external capsules, thalamus, and basal ganglia were involved, better anatomic delineation was seen on proton density-weighted images. When a lesion is near a ventricle or subarachnoid space, the presence of CSF makes it difficult to identify the lesion on T2-weighted images since the signal intensities of CSF and the lesion may be similar.

On both initial and follow-up scans, T1-weighted images are the least sensitive for detection of stroke. This is not unexpected owing to the negative mix of T1 and proton-density effects [23].

Our results show a larger infarct, increased signal intensity on proton density- and T2-weighted images, and increased radiolucency on CT on follow-up examinations in approxi-

mately 30% of cases (seven of 20 on the basis of MR size criteria). These are important findings, although not surprising. In addition, 15% of lesions (three of 20) "appeared" between the first and second MR examinations. Thus, despite the sensitivity of MR in the detection of early ischemia, dynamic events occur between the first 24 hr and the subacute follow-up. The significance of this finding is the implication of a larger tissue area "at risk" that is not currently identified on routine

MR scans. Explanations for this change in lesion size include infarct extension into the "penumbra," lysis of proximal emboli with reperfusion and/or distal embolization, and spread of secondary edema. Additional clinical, perfusion, metabolic, and angiographic studies are required to determine the precise pathogenesis of these lesions [24–26].

These human clinical results are in keeping with previous reports on the MR appearance of infarction [17–20, 27],

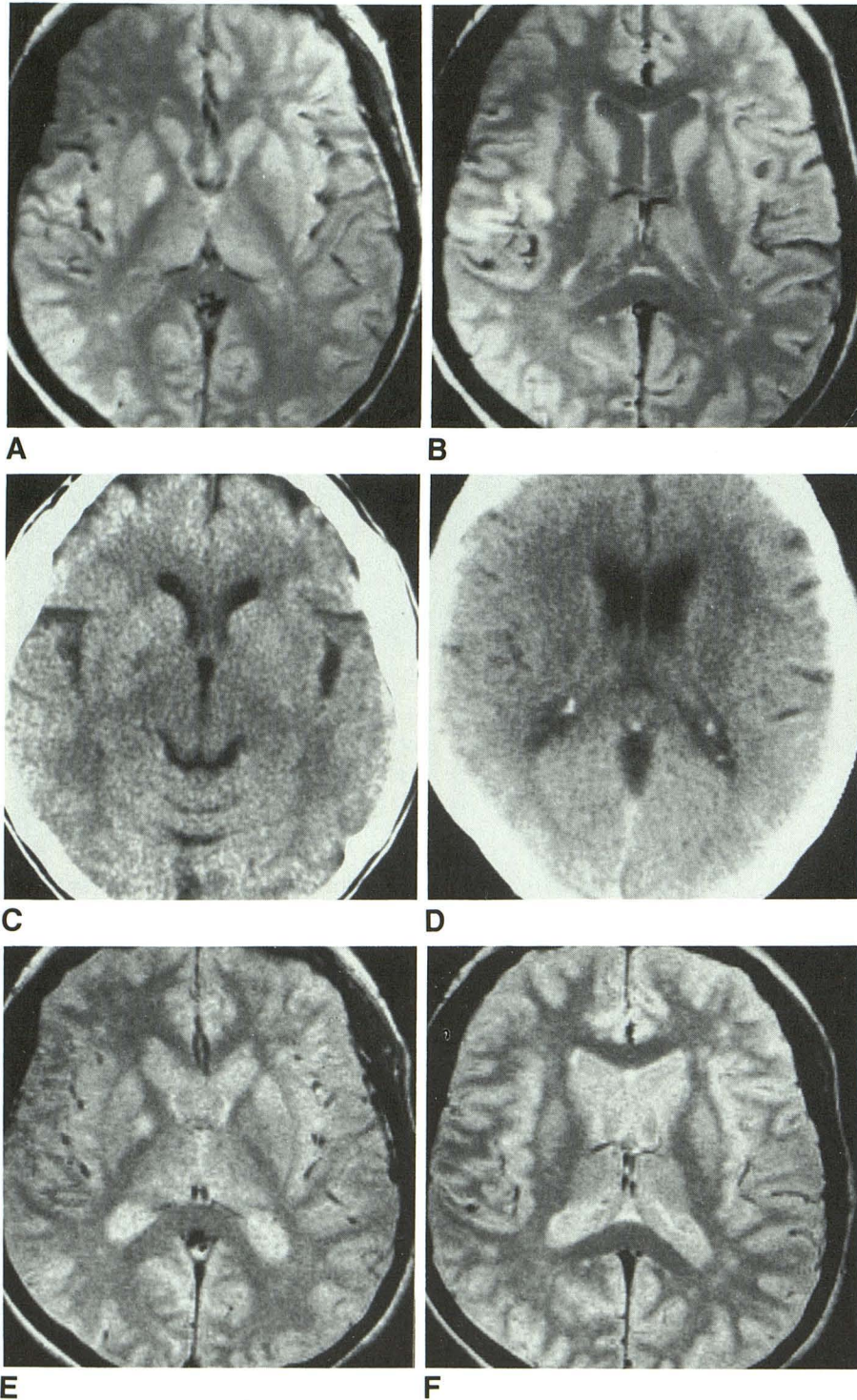


Fig. 6.—Right basal ganglia infarct and apparent right temporal cortical infarct on day 1 (A and B) with resolution of right cortical findings on follow-up examination on day 7 (C–F). Initial CT study was normal.

A and B, Proton density-weighted MR images (3000/35), show right basal ganglia and right temporal cortical infarct.

C and D, CT now shows infarct in right basal ganglia.

E and F, Proton density-weighted MR images (3000/35) show right basal ganglia infarct and resolution of changes in right temporal cortex.

although this earlier work primarily relates to older lesions. Animal experiments indicate that signal changes on conventional spin-echo MR images occur 2–4 hours after ischemic insult [11, 12, 15]. None of our patients was scanned earlier than 4 hr after ictus, but one might not expect to see abnormal MR scans in patients scanned before this time [16].

We believe MR is the most sensitive, accurate, and practical means of imaging acute stroke. However, the significance of the signal changes as well as their relationship to the pathophysiology of acute stroke needs to be clarified. We postulate that the early changes observed on MR reflect changes in intracellular water arising from loss of normal energy homeostasis, subsequent membrane dysfunction (particularly sodium-potassium pumps), increase in intracellular water, associated diminished binding of water, and consequent increase in T1 and T2 [28–32].

In only one case (Fig. 6) did an anatomic region of abnormal MR signal intensity revert to normal. However, our study excluded patients with transient ischemic attacks, and, therefore, we may have underestimated the number of patients in whom MR signal-intensity changes were transient.

Another critical factor in the diagnosis and current management of acute stroke is determination of the presence of a hemorrhagic component. Our results indicate that in the earlier stages of stroke, CT and MR may be equally suited to diagnosing hemorrhage. In the two cases of obvious acute hematoma in our series, typical changes of increased radiodensity on CT and decreased signal intensity on T2 and GRE MR scans were seen (Fig. 2). However, the number of cases of acute hemorrhage in this study is small, and other reports have indicated that acute hemorrhage may not be as obvious on MR as on CT, particularly if GRE scans are not obtained [33]. On the basis of published reports, it is probably not inappropriate to continue to obtain CT scans in the setting of acute stroke, although we believe that more experience with GRE imaging will obviate additional studies [34].

The other main finding related to hemorrhage in stroke is its comparative frequency, as reflected by increased signal intensity on T1-weighted images (Figs. 3 and 4). This type of hemorrhagic signal intensity was seen on follow-up (six of 20) as well as on a few initial (two of 31) MR scans. This hemorrhagic pattern differs from that of the usual hematoma. In particular, it is not associated with decreased signal intensity on T2-weighted images, nor are T2* effects reflected by decreased signal intensity on GRE images. Furthermore, the presence of "methemoglobin" (increased T1-weighted signal intensity) signal on the first day of ischemia is not in keeping with the usual 3- to 4-day process of oxidation of hemoglobin to methemoglobin [35]. These are not frank hematomas, but ischemic lesions with damaged capillary endothelium through which there is leakage, including diapedesis of RBCs, into the surrounding parenchyma; that is, ischemic petechial infarction.

These results suggest that MR offers important capabilities for the clinical evaluation as well as investigation of acute stroke. MR appears to detect ischemic stroke at an earlier stage than CT does and better defines its extent. It also allows differentiation of any associated hemorrhage.

ACKNOWLEDGMENTS

We thank Sharon Norman for data collection and collation and Marge Eddy for manuscript preparation.

REFERENCES

1. Brant-Zawadzki, Weinstein P, Bartkowski H, Moseley M. MR imaging and spectroscopy in clinical and experimental cerebral ischemia: a review. *AJR* **1987**;148:579–588
2. Kricheff IJ. Arteriosclerotic ischemic cerebrovascular disease. *Radiology* **1987**;162:101–109
3. Welch KMA, Levine SR, Ewing JM. Viewing stroke pathophysiology: an analysis of contemporary methods. *Stroke* **1986**;17(6):1071–1077
4. Hachinski V, Norris JW. *The acute stroke*. Philadelphia: Davis, **1985**
5. Inoue Y, Takemoto K, Miyamoto T, et al. Sequential computed tomography scans in acute cerebral infarction. *Radiology* **1980**;135:655–662
6. Hakim AV, Rynder-Cooke A, Melanson D. Sequential computerized tomographic appearance of strokes. *Stroke* **1983**;14:893–897
7. Wall SD, Brant-Zawadzki M, Jeffrey RB, Barnes B. High frequency CT findings within 24 hours of cerebral infarction. *AJR* **1982**;138:307–311
8. Tomura N, Uemura K, Inugami A, et al. Early CT finding in cerebral infarction: obscuration of the lentiform nucleus. *Radiology* **1988**;168:463–467
9. Bushnell DL, Gupta S, Mlcoch AG, Romyn A, Barnes WE, Kaplan E. Demonstration of focal hyperemia in acute cerebral infarction with iodine-123 iodoamphetamine. *J Nucl Med* **1987**;28:1920–1923
10. Wise RJS, Rhodes CG, Gibbs JM, et al. Disturbance of oxidative metabolism of glucose in recent human cerebral infarcts. *Ann Neurol* **1983**;14:627–637
11. Bose B, Jones SC, Lorig R, Friel HT, Weinstein M, Little JR. Evolving focal cerebral ischemia in cats: spatial correlation of nuclear magnetic resonance imaging, cerebral blood flow, tetrazolium staining, and histopathology. *Stroke* **1988**;19:28–37
12. Brant-Zawadzki M, Pereira B, Weinstein P, et al. MR imaging of acute experimental ischemia in cats. *AJNR* **1986**;7:7–11
13. Gadian DG, Frackowiak SJ, Crockard HA, et al. Acute cerebral ischaemia: concurrent changes in cerebral blood flow, energy metabolites, pH, and lactate measured with hydrogen clearance and ³¹P and ¹H nuclear magnetic resonance spectroscopy. I. Methodology. *J Cereb Blood Flow Metab* **1987**;7(2):199–206
14. Komatsumoto S, Nioka S, Greenberg JH, et al. Cerebral energy metabolism measured in vivo by ³¹P-NMR in middle cerebral artery occlusion in the cat—relation to severity of stroke. *J Cereb Blood Flow Metab* **1987**;7:557–562
15. Kucharczyk J, Chew W, Derugin N, et al. Nicardine reduces ischemic brain injury: magnetic resonance imaging/spectroscopy study in cats. *Stroke* **1989**;20:268–273
16. Yuh WTC, Crain MR, Loes DJ, Greene GM, Ryals TJ, Sato Y. MR imaging of cerebral ischemia: findings in the first 24 hours. *AJNR* **1991**;12:621–629
17. Biller J, Adams HP, Dunn V, Simmons Z, Jacoby CG. Dichotomy between clinical findings and MR abnormalities in pontine infarction. *J Comput Assist Tomogr* **1986**;10(3):379–385
18. Brown JJ, Hesselink JR, Rothrock JF. MR and CT of lacunar infarcts. *AJNR* **1988**;9:477–482
19. Bryan RN, Willcott MR, Schneiders NJ, Ford JJ, Derman HS. Nuclear magnetic resonance evaluation of stroke. *Radiology* **1983**;149:189–192
20. DeWitt LD, Kistler JP, Miller DC, Richardson EP, Buonanno FS. NMR-neuropathologic correlation in stroke. *Stroke* **1987**;18(2):342–351
21. Imakita S, Nishimura T, Naito H, et al. Magnetic resonance imaging of human cerebral infarction: enhancement with Gd-DTPA. *Neuroradiology* **1987**;29:422–429
22. Simmons Z, Biller J, Adams HP, Dunn V, Jacoby CG. Cerebellar infarction: comparison of computed tomography and magnetic resonance imaging. *Ann Neurol* **1986**;19(3):291–293
23. Bryan RN, Weathers SW, Blackwell RD. Central nervous system magnetic resonance imaging. In: Appel SH, ed. *Current neurology*. Chicago: Year Book Medical, **1988**:251–294
24. LeBihan D, Breton E, Lallemand D, et al. Separation of diffusion and

- perfusion in intravoxel incoherent motion MR imaging. *Radiology* **1988**;168:497-505
25. Grotta JC. Can raising cerebral blood flow improve outcome after acute cerebral infarction? *Stroke* **1987**;18:264-267
 26. Figols J, Cervos-Navarro J, Sampaolo S, Ferszt R. Microthrombi in the development of ischemic irreversible brain infarct. In: Cervos-Navarro J, Ferszt R, eds. *Stroke and microcirculation*. New York: Raven, **1987**: 69-74
 27. Miyashita K, Naritomi H, Sawada T, et al. Identification of recent lacunar lesions in cases of multiple small infarctions by magnetic resonance imaging. *Stroke* **1988**;19:834-839
 28. Erecinska M, Silver IA. ATP and brain function. *J Cereb Flood Flow Metab* **1989**;9:2-19
 29. Symon L, Wang A, Momma F. Aspects of cerebral ischemia in humans: clinical correlates of primate thresholds. In: Cervos-Navarro J, Ferszt R, eds. *Stroke and microcirculation*. New York: Raven, **1987**:1-4
 30. Plum F. What causes infarction in ischemic brain. The Robert Wartenberg lecture. *Neurology* **1983**;33:222-233
 31. Mano I, Levy RM, Crooks LE, Hosobuchi Y. Proton nuclear magnetic resonance imaging of acute experimental cerebral ischemia. *Invest Radiol* **1983**;17:345-351
 32. Eleff SM, Schnall MD, Ligetti L, et al. Concurrent measurements of cerebral blood flow, sodium lactate, and high-energy phosphate metabolism using ^{19}F , ^{23}Na , ^1H , and ^{31}P nuclear magnetic resonance spectroscopy. *Magn Reson Med* **1988**;7:1-13
 33. Edelman RR, Johnson K, Buxton R, et al. MR of hemorrhage: a new approach. *AJNR* **1986**;7:751-756
 34. Zyed A, Hayman LA, Bryan RN. MR imaging of intracerebral blood: diversity in the temporal pattern at 0.5 and 1.0 T. *AJNR* **1991**;12:469-474
 35. Gomori JM, Grossman RI, Yu Ip C, Asakura T. NMR relaxation times of blood: their dependence on field strength, oxidation state, and cell integrity. *J Comput Assist Tomogr* **1987**;11:684-690